minerals

MDPI

Article

Optical and Electronic Microscope for Minero-Petrographic and Microchemical Studies of Lime Binders of Ancient Mortars

Emma Cantisani [1,*], Fabio Fratini [1] and Elena Pecchioni [1,2]

[1] CNR-ISPC-Institute of Heritage Science (Florence Unit), Via Madonna del Piano, 10, 50019 Sesto Fiorentino, Florence, Italy; fabio.fratini@cnr.it (F.F.); elena.pecchioni@unifi.it (E.P.)
[2] Earth Sciences Department, University of Florence, Via G. La Pira 4, 50121 Florence, Italy
* Correspondence: emma.cantisani@cnr.it

Abstract: In this paper, the advances in the use of optical and electronic microscope for study of the minero-petrographic and microchemical features of lime binders of ancient mortars are discussed for various case studies. Mortars belonging to several historic periods and with different functions in building structures and archaeological sites were selected in order to verify the complementarity of optical and electronic microscope analyses applied to these artificial materials. The data obtained with the application of optical and microscope analyses were able to provide detailed and more precise information on the composition, structure, and texture of lime binders, highlighting the features of air hardening calcitic lime binder, air hardening magnesian lime binder, natural hydraulic lime binder, and air hardening binders with materials providing hydraulic characteristics added. Furthermore, a complete analysis and classification of the lime lumps was determined.

Keywords: ancient mortar; binder; lime; optical and electronic microscope

Citation: Cantisani, E.; Fratini, F.; Pecchioni, E. Optical and Electronic Microscope for Minero-Petrographic and Microchemical Studies of Lime Binders of Ancient Mortars. *Minerals* **2022**, *12*, 41. https://doi.org/10.3390/min12010041

Academic Editors: Adrián Durán Benito and Anna Arizzi

Received: 11 November 2021
Accepted: 22 December 2021
Published: 28 December 2021

1. Introduction

Mortars, one of the oldest building materials, perform an essential function in architecture, namely that of binding together loose materials and thus allowing the production of any type of building structure.

The choice of raw materials (limestone, marly limestone, gypsum, and so on) for the manufacture of binders and the selection of aggregates (i.e., sand), additives, and admixtures able to confer specific properties for each construction purpose is the result of considerable technological knowledge.

The use of mortars has progressed, differing in an extraordinary way over time: from the ceilings of the tombs of pre-dynastic Egypt to the *opus caementicium* that distinguishes Roman architecture; from the succession of layers, necessary for the drafting of a mural painting, to those for the laying of a floor of stone slabs or mosaic tiles; and from the stucco ornaments of the Baroque and *Rococò* to the Portland cement of the "artificial stones" of Liberty, up to the reinforced concrete [1,2].

The information contained in the mortars allows to recognize the ancient "recipes" identifying the main constituents such as the aggregate and binder; the latter being the ingredient that has the function to give "cohesion" to the paste, hardening it. In this sense, it is the main factor that can contribute to the performances and durability of these materials.

Archaeological studies [3–5] have revealed that the first binder used by man was clay, which, although widely used and widespread over the centuries, nevertheless remained unsuitable for realizing more solid constructions or support surfaces for decorations or mural paintings. Empirical experience made it possible to discover binders with significantly better performances thanks to the accidental burning, at high temperatures, of different types of carbonate and chalky rocks. The difference among the various binders is based on the capability, once mixed with water, to harden in the air or in a humid environment. Hence the subdivision into air binders and hydraulic binders. The cohesive action develops

through the setting reaction, which is different depending on the type of binder. Below, the main inorganic binders analyzed in this paper are summarized:

- air hardening calcitic lime (lime putty, hydrated lime in powder) obtained by burning pure limestones at temperatures of 800–950 °C—it sets by carbonation in the air of calcium hydroxide with the formation of calcite;
- air hardening magnesian lime (lime putty) obtained by burning dolomitic limestone or dolomite at temperatures of 800–950 °C—it sets by carbonation of the calcium hydroxide and by partial carbonation of magnesium hydroxide with formation of hydromagnesite;
- air hardening calcitic lime with materials providing hydraulic characteristics added, namely compounds based on active silica and alumina (i.e., in the amorphous state). They set even in conditions of high humidity partly by carbonation of calcium hydroxide and partly by reaction of calcium hydroxide with the hydraulic components and formation of hydrated calcium silicates and hydrated calcium aluminates. Among these compounds, we remember pozzolana, crushed bricks, ground ceramic products, diatomaceous earth, metakaolin, and blast furnace slags;
- historical natural hydraulic limes, obtained with traditional manufacturing, burning weakly marly limestone (content of clay between 6.5–20%) [6,7] or siliceous limestone, at temperatures of 800–950 °C—they set even in conditions of high humidity, partly for the carbonation of calcium hydroxide and partly for the formation of hydrated calcium silicates and aluminates.

Among the types of binders, modern hydraulic binders (natural cement, Portland cement, and so on) should also be mentioned, first produced in the mid-19th century, as well as ancient gypsum binders, which, however, will not be treated in this work, as it is restricted only to lime mortars [8].

Historical Background on the Study of Mortars

Mortars can be compared to "lithic" materials, like, for example, sandstones, as they derive from stone materials, resembling them and behaving as such. In fact, they are composed of a binder fraction, an aggregate, and possible additives/admixtures. It is thus clear that only an adequate characterization (petrographic, mineralogical, chemical, and physico-mechanical) provides information on the nature of these "ingredients", allowing a correct classification of the mortars themselves. However, until the early 1980s, the study of historical mortars was mainly based on traditional wet chemical analyses [9–12]. The data obtained with this type of investigation provided extremely partial information, as in the case when the binder and the aggregate have the same chemical nature (i.e., carbonate aggregate). Considering this, it was clear that a correct study had to examine the petrographic and mineralogical characteristics through a thin section study under a polarizing optical microscope, as if the mortars were a completely natural compound similar to a rock [8,13–16]. Specifically, the choice of the most appropriate analytical techniques essentially depends on the questions to be answered as well as on the amount of material available [17–20].

There are at least three distinct sectors that require a different study approach: (a) conservation of historical monuments, (b) the archaeological sector, and (c) the research sector [7,21]. In the context of conservation, information on the composition of ancient mortars with the purpose of understanding the decay phenomena and to formulate restoration mortars compatible with the materials and environmental conditions present is required [22–24]. The archaeological sector is mainly interested in the dating of the masonries, origin of raw materials, technologies for the realization of the mixtures, and contribution to the knowledge of the construction phases. The data obtained must also make it possible to obtain information on the socio-economic conditions existing at the time of manufacturing [25–29]. The research sector is mainly aimed at understanding the factors that have contributed to the particular durability of a mortar, with the aim of developing new types of binders and mortars [30–36].

The aim of this paper is to prove and highlight the advantages in the complementary use of optical and electronic microscope for a minero-petrographic and morphological and microchemical characterization of lime binders of ancient mortars. Mortars, belonging to several periods, with different functions in historic buildings and archaeological sites, were selected as case studies. The characterization of binders, carried out by means of optical and electronic microscope, provides information on their composition, structure, and texture, being able to distinguish among the use of air hardening calcitic lime binder, air hardening magnesium lime binder, natural hydraulic lime binder, and air hardening binders with materials providing hydraulic characteristics added. Furthermore, a detailed analysis and classification of the lime lumps is presented, as well as components that can provide information on the binder and mixture production process and are also able to indicate which kind of carbonate stone was used to produce the lime.

The different characteristics of mortars, in terms of raw materials and technologies used for the preparation of mixture and application in the masonries, can then provide important information on material culture.

2. Materials and Methods

In Table 1, a brief description (function, localization age, and type) of the mortars and performed analyses is reported.

The minero-petrographic observations were carried out on the thin sections (30 μm) of samples by means of a PLM ZEISS Axio Scope A1 microscope (Carl Zeiss, Jena, Germany), with video camera, resolution of 5 megapixels, and image analysis software Axio Vision (V1).

The minero-petrographic study of the mortars through polarized light microscope (PLM) allows to highlight the following aspects of the binder:

- the mineralogical composition;
- the birefringence color;
- the texture (micritic, microsparitic, sparitic recrystallizations);
- the structure (homogeneous, presence of patches, and so on);
- interactions with the aggregate (e.g., reaction edges);
- the presence of neoformation phases;
- the aspect of macropores;
- the presence of lumps.

The presence of the lumps that macroscopically show a whitish color and often a low consistency [8,37,38], indicate a production of the lime according to a traditional technology, involving the slaking of the quicklime clods with excess water in order to obtain a white paste (lime putty). The characterization of lumps through optical and electronic microscope can help in the classification of the binders, in the identification of carbonate stone used for the production of lime, and in the identification of some "defects" in the manufacturing technologies [39].

Morphological and semi-quantitative microchemical analyses were obtained by means of an SEM EDS electronic microscope (ZEISS EVO MA 15) (Carl Zeiss, Jena, Germany) with W filament equipped with an analytical system in the dispersion of energy EDS/SDD, Oxford Ultimax 40 (40 mm^2 with resolution 127 eV @5.9 keV) (Oxford Instruments, Abingdon, UK) with Aztec 5.0 SP1 software.

The measurements were performed on carbon metallized thin sections of the samples on binder and lumps with the following operating conditions: an acceleration potential of 15 kV, 500 pA beam current, working distance comprised between 9 and 8.5 mm; 20 s live time as acquisition rate useful to archive at least 600,000 cts, on Co standard, and process time 4 for point analyses; and 500 μs pixel dwell time for maps acquisition with 1024 × 768 pixel resolution.

The software used for the microanalysis was an Aztec 5.0 SP1 software that employs the XPP matrix correction scheme developed by Pouchou and Pichoir in 1991 [40]. This is a Phi-Rho-Z approach that uses exponentials to describe the shape of the φ (ρz) curve.

XPP matrix correction was chosen because of its favorable performance in situations of severe absorption such as the analysis of light elements in a heavy matrix. The procedure is a "standard-less" quantitative analysis that employs pre-acquired standard materials for calculations. The monitoring of constant analytical conditions (i.e., filament emission) is archived with repeated analyses of a Co metallic standard.

The SEM EDS morphological and chemical study allowed to highlight and characterize the typology of binder and the kind of lumps.

Table 1. Description of the mortars and performed analyses.

Localisation/Age	Function Type	Analyses Carried Out
1. Dome of the Florence Cathedral (15th century)	Bedding mortar	PLM/SEM
2. San Martino Fortress, Mugello-Florence (16th century)	Bedding mortar	PLM/SEM
3. Bridge in the St. Baume massif, Provence-France (18th century)	Bedding mortar	PLM/SEM
4. Bridge in the St Baume massif, Provence-France (18th century)	Bedding mortar	PLM/SEM
5. Genoa city walls (14th century)	Bedding mortar	PLM/SEM
6. Core of a pillar, Augusto bridge, Narni-Terni (1st century BC)	Filling mortar	PLM/SEM
7. Wall set against the *cella*, Sanctuary of Apollo, Building A in Hierapolis archaeological site, Denizli (Turkey), Proto-Byzantine age	Bedding mortar	PLM/SEM
8. Camponeschi Palace L'Aquila (18th century)	Bedding mortar	PLM/SEM
9. Roman tank in Carsulæ Terni (1st century AD)	Bedding mortar	PLM/SEM
10. Masonry mortar of Del Trebbio Castle Mugello-Florence (15th century)	Bedding mortar	PLM/SEM
11. Davanzati Palace Florence (14th century)	Bedding mortar	PLM/SEM
12. Florentine county house of the 19th century	Bedding mortar-lump	PLM
13. Luni Roman theatre (1st century AD)	Bedding mortar-lump	PLM
14. Ambulatio of Torraccia di Chiusi archaeological site (second half of 4th century AD)	Bedding mortar-lump	PLM
15. San Francesco Church (Pisa) 13–17th century	Bedding mortar-lump	PLM
16. San Francesco Church (Pisa) 13–17th century	Bedding mortar-lump	
17. Roman aqueduct, Quarto, Florence (1st–2th century AD)	Bedding mortar	PLM/SEM
18. Roman findings, Spello, Umbria (1st century AD)	Bedding mortar	PLM/SEM

3. Results and Discussion

3.1. Air Hardening Calcitic Lime

As previously reported, the air hardening calcitic lime is obtained by burning pure limestones. The variables influencing the microscopic characteristics of the binder are numerous: type of limestone, production procedures, as well as dissolution and recrystallization processes occurring over time. In the preparation of an air hardening calcitic lime, different types of limestones can be used: more or less pure micritic limestones (with clay

and silica impurities, iron oxides and so on), crystalline carbonates (marbles, travertines), and organogenic limestones. During burning, the presence of impurities acts as a catalyst for the dissociation of calcium carbonate, which is then obtained at a lower temperature. This allows to have small calcium oxide crystals and, as a consequence, small crystals of calcium hydroxide during slaking. These crystals can carbonate quickly, determining a micritic texture of the binder. The burning of pure non-porous crystalline limestones, such as marble, occurs with the formation of coarser calcium oxide crystals. This, after hydration, gives rise to large hydroxide crystals, determining slower carbonation and a final texture of the binder that tends to be microsparitic. Furthermore, concerning the production process, a high burning temperature (above 1000 °C) causes sintering processes of calcium oxide with the formation of large crystals and a final microsparitic binder texture. Even over time, the exposure of the masonry to atmospheric agents can cause dissolution and re-precipitation phenomena in the mortar binder, which can sometimes cause its complete recrystallization [7,41,42].

The combined use of optical and electronic microscope allowed us to identify the texture of an air hardening calcitic lime, the type of burned limestone, the manufacturing technologies, and the possible dissolution/recrystallization phenomena.

Figure 1a,b refer to a mortar taken from the core of the masonry of the dome of the Florence Cathedral (15th century). The typical features of this type of binder are as follows: homogeneous appearance and micritic texture consisting of calcite crystals with dimensions of less than 10 μm. The color in cross polarized light is light brown and is a function of the interference color of the calcite, which is of the third order (birefringence = 0.154–0.1740) (Figure 1a). The micritic aspect of binder is also confirmed by high magnification image using an SEM microscope (Figure 1b). It is a mortar made of an air hardening calcitic lime binder obtained by burning a micritic limestone with clay impurities <6.5%, as suggested by remains in a thin section of under-burnt rock fragments of Pietra Alberese, the limestone used in the Florentine territory for the production of lime [43].

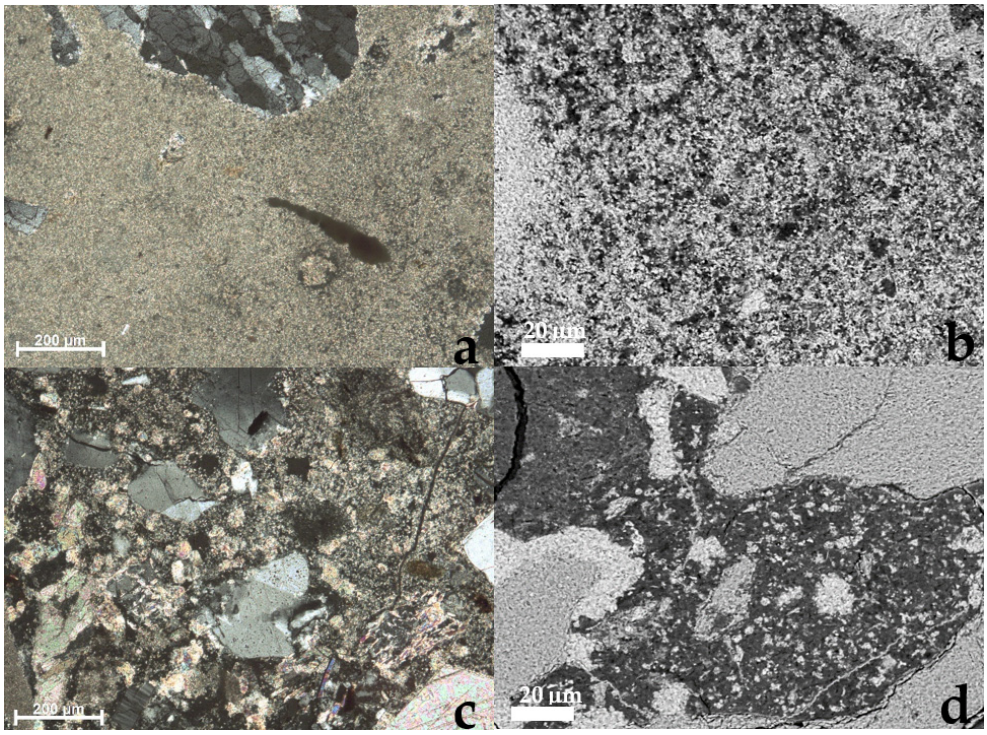

Figure 1. Microphotographs of air hardening calcitic lime binder: (**a**) micritic texture under PLM, xpl, and (**b**) SEM image at high magnification (dome of the Florence Cathedral (15th century)); (**c**) sparitic texture under PLM, xpl, and (**d**) SEM image at high magnification (Medici Fortress of San Martino in San Piero a Sieve (Mugello, Tuscany, 16th century). The length of the bar in the SEM images is 20 μm.

Figure 1c refers to a mortar taken from the core of the masonry of the Medici Fortress of San Martino in San Piero a Sieve (Mugello, Tuscany 16th century). This binder was also produced by burning a micritic limestone with small clay impurities (Pietra Alberese), but the original micritic structure is completely transformed into sparite for dissolution and slow crystallization phenomena, probably owing to the particular environmental conditions (RH%) in which these wall structures were found. The sparitic aspect of some area of binder is evident in the high magnification image using an SEM microscope (Figure 1d).

3.2. Air Hardening Magnesian Lime

This type of lime, obtained by burning dolomitic limestone or dolomite, is characterized by non-homogeneity owing to segregation phenomena of the magnesium phases. Indeed, magnesium hydroxide (brucite), owing to the lower carbonation rate compared with calcium hydroxide, is concentrated in patches located in the areas of the mortar where water stagnates, providing characteristic almost similar to a hydraulic mortar. Moreover, residual phases of magnesium hydroxide remain non-carbonated [7,8]. The coupling of observation of thin sections under PLM and morphological and micro-chemical analyses with SEM EDS allows the identification of these segregation phenomena inside the binder and a semi-quantitative analysis of the new developed mineralogical phases. Figure 2a shows the microscopic aspect of the bedding mortar of a small bridge located in a rural area of the Sainte Baume massif in Provence (18th century). The binder has a micritic texture free from impurities. The diagnostic feature that allows us to recognize that this binder was obtained by burning dolomitic or magnesium carbonate rocks is the sporadic presence of subspherical elements with an opaque appearance and size less than 100 µm. The SEM EDS maps (Figure 2b,c) of Ca and Mg show clearly the segregation of the two phases; Mg phases are more concentrated in the subspherical elements, testifying their origin from unmixing remains of Ca and Mg phases. The subspherical elements contain MgO ranging from 84.50 to 51.90 %, CaO from 13.23 to 46.48, Al_2O_3 from 4.29 to 1.62, and Fe_2O_3 from 0.35 to 0.87 (see Table 2).

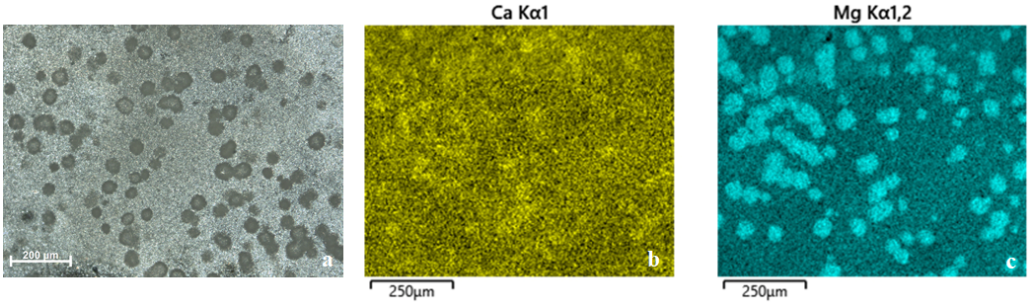

Figure 2. Microphotographs of subspherical elements in an air hardening magnesian lime coming from a bedding mortar of a small bridge located in a rural area of the Sainte Baume massif in Provence (18th century) (**a**) under PLM, xpl, (**b**) SEM EDS map of Ca, and (**c**) SEM EDS map of Mg.

Table 2. Microchemical spot analyses (SB1–SB7) of subspherical elements in the binder of Figure 2.

Oxides %	SB1	SB2	SB3	SB4	SB5	SB6	SB7
Na_2O	bdl	bdl	bdl	bdl	bdl	bdl	bdl
MgO	59.53	77.71	76.72	59.85	84.5	51.9	74.01
Al_2O_3	2.69	2.77	2.65	4.29	2.30	1.62	2.56
SiO_2	bdl	bdl	bdl	bdl	bdl	bdl	bdl
SO_3	bdl	bdl	bdl	bdl	bdl	bdl	bdl
CaO	37.16	19.52	20.36	34.83	13.23	46.48	23.43
Fe_2O_3	0.35	bdl	0.87	0.8	bdl	bdl	bdl
NiO	bdl	bdl	bdl	bdl	bdl	bdl	bdl

bdl: below detection limit.

In Figure 3a, always referable to the mortar of the small Provençal bridge of Sainte Baume massif, crystallizations of hydromagnesite are visible, identified in PLM by the radiated fibrous structure and by the first-order grey interference color, concentrated in the porosity and area of preferential stagnation of the mixing water. The microchemical map (SEM EDS) of the fibrous needles in a radial shape shows a high Mg content, confirming the presence of hydromagnesite (Figure 3b).

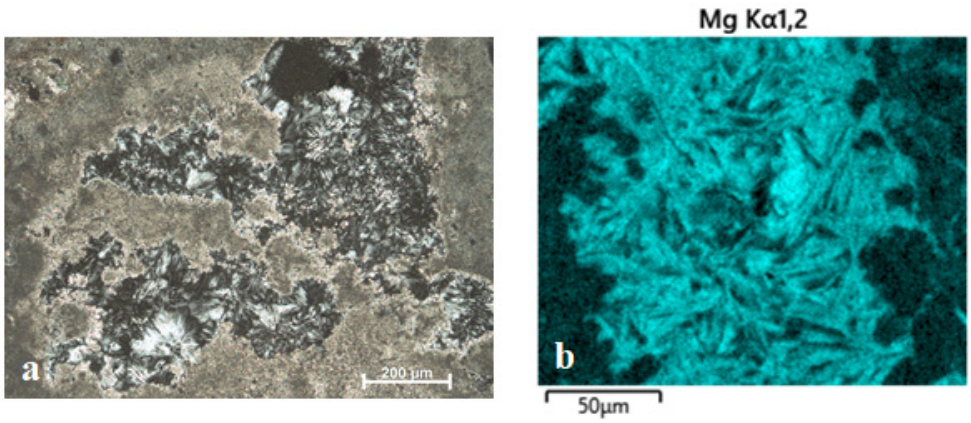

Figure 3. Microphotographs of hydromagnesite crystals in an air hardening magnesian binder of a bedding mortar belonging to a small bridge located in a rural area of the Sainte Baume massif in Provence (18th century) under (**a**) PLM, xpl, and (**b**) a particular SEM EDS map of Mg.

Figure 4a refers to a mortar of the core of the masonry of a bastion of the 14th century city walls of Genoa, which macroscopically shows a particularly white binder and very strong cohesion. A micritic-textured binder is observed with PLM in which newly formed crystals with dimensions of about 40 µm and high birefringence color are homogeneously diffused, as well as darker areas in the binder. The microchemical analysis highlighted that the area with high birefringence color in PLM is enriched in Ca, while the darker thickenings are enriched in Mg (Figure 4b). The MgO amount ranges from 9.80% to 43.16%, showing a strong variability of composition of binder (see Table 3). Therefore, the chemical data and petrographic observations confirm a segregation of Ca and Mg during the setting of the binder.

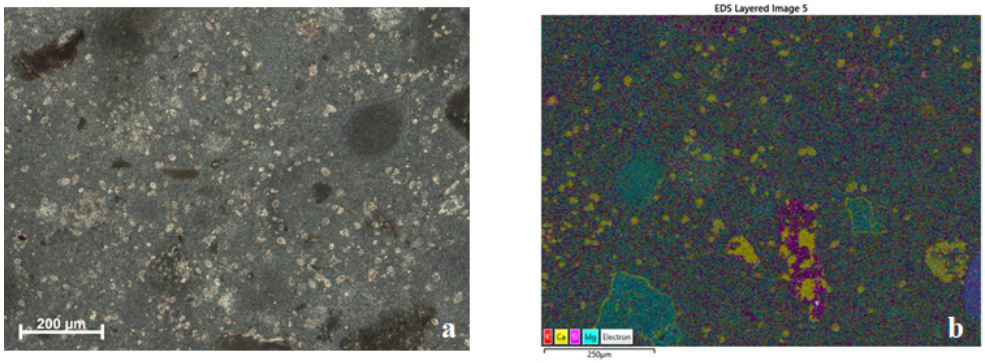

Figure 4. Microphotographs of high birefringence and dark areas in the binder of an air hardening magnesian lime belonging to a mortar of the core of the masonry of a bastion of the 14th century city walls of Genoa under (**a**) PLM, xpl, and (**b**) SEM EDS layered map of K, Ca, Mg, and Si.

Table 3. Microchemical spot analyses (GP1–GP7) of high birefringence and dark areas of air hardening magnesian lime of Figure 4.

Oxides %	GP1	GP2	GP3	GP4	GP5	GP6	GP7
Na_2O	0.38	0.23	0.07	bdl	0.25	0.38	0.37
MgO	26.89	9.80	12.67	37.62	43.16	37.7	40.38
Al_2O_3	1.15	0.26	0.19	1.30	8.70	1.03	7.65
SiO_2	19.56	6.70	5.67	23.83	23.42	23.07	22.67
SO_3	0.45	0.07	0.16	0.37	bdl	0.44	0.82
CaO	50.83	82.62	80.88	36.81	24.11	37.39	26.74
Fe_2O_3	0.75	0.11	0.12	0.07	0.35	bdl	1.19
NiO	bdl	0.23	0.24	bdl	bdl	bdl	0.18

bdl: below detection limit.

3.3. Air Hardening Calcitic Lime with Materials Providing Hydraulic Characteristics

The materials with pozzolanic behavior are numerous and recognizable under the optical microscope in transmitted light (PLM). Some are deliberately added, such as tuff, pumice, volcanic ash, crushed bricks, diatomaceous earth (diatomite), forging slag, foundry slag, fired kaolin, fired clay, and so on, whereas others are randomly present in the aggregate [44–46]. Among the latter, the most reactive is microcrystalline silica (flint), as can be observed in the mortar of the core of the pillar of the Augusto bridge near Narni (27 BC), where a reaction rim is clearly visible (Figure 5a,b) [41]. The microchemical analysis shows in detail the composition of the rim, confirming the presence of an amount of Si higher than 50%. In Table 4, the microchemical analyses performed on the reaction rim in the area (spectrum 1), in spots (spectrum 3, 4, 5), and in the binder (spectrum 6) are reported (for the position, see Figure 5c). The HI index, calculated as (SiO_2 + Al_2O_3 + Fe_2O_3)/(CaO + MgO) [7], ranges from 1.6 to 0.81, confirming the very high hydraulicity of the mortar, responsible for the strong durability of this material.

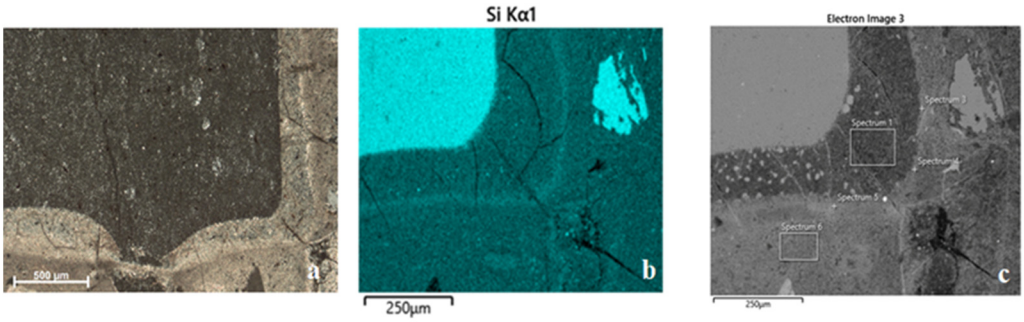

Figure 5. Microphotographs of reaction rim of microcrystalline silica (flint) in the mortar of the core of the pillar of the Augusto bridge near Narni (27 BC) under (**a**) PLM, xpl, and (**b**) EDS map of Si and and (**c**) BS image with reported areas and spots analyzed with EDS (for results, see Table 4).

Table 4. Microchemical analyses of reaction rim portions and binder of Narni sample.

Oxides %	Spectrum 1	Spectrum 3	Spectrum 4	Spectrum 5	Spectrum 6
Na_2O	2.13	1.25	1.28	1.22	1.50
MgO	bdl	bdl	bdl	bdl	0.59
Al_2O_3	4.88	3.91	3.15	2.58	2.38
SiO_2	52.34	52.96	55.67	40.90	42.92
SO_3	bdl	0.78	bdl	bdl	bdl
K_2O	1.40	0.85	0.72	0.83	0.72
CaO	36.49	39.48	38.24	53.57	50.69
Fe_2O_3	1.07	bdl	bdl	bdl	bdl

bdl: below detection limit.

Nevertheless, reaction rims have also been observed in the presence of shale and arenaceous fragments containing shale [47–49]. This can be explained because clay minerals can contain amorphous SiO_2 and Al_2O_3 (owing to the thermal activation during diagenesis and metamorphism).

According to St. John et al. (1998) [50], from the chemical point of view, the reactive constituents present in the hydraulic additions are substantially of three types: amorphous silica, amorphous silico-aluminates, and aluminum silicates altered to zeolitic structure. Hence, different types of pozzolanic behavior materials develop the same type of CSH (calcium silicate hydrate). Charola and Henrique (1999) [51] cite prehnite, gehlenite, diopside, analcime, leucite, and melilite as newly formed minerals produced in the lime–pozzolan reaction. It must be said that the most common hydraulic compounds such as pozzolan and crushed brick or cluster of fired clay, unintentionally found in the mixture, normally develop reaction rims on the side of the carbonate binder. However, the grain size of these component splays a fundamental role; this is the case of the bedding mortars of the wall set against the *cella* in Building A of Sanctuary of Apollo, in Hierapolis archaeological site (Denizli—Turkey) (Proto-Byzantine age) [52]. The large dimensions of the crushed bricks (Figure 6a), as evidenced in PLM observation, prevented the development of high hydraulicity. In Figure 6b, the layered maps of Ca, Si, Al, and Mg show a lower amount of Si and Al in the rim developed between crushed brick and binder. The relative microchemical analyses are reported in Table 5 and the calculated HI for the rim areas ranges from 0.25 to 0.30, evidencing a medium hydraulicity value.

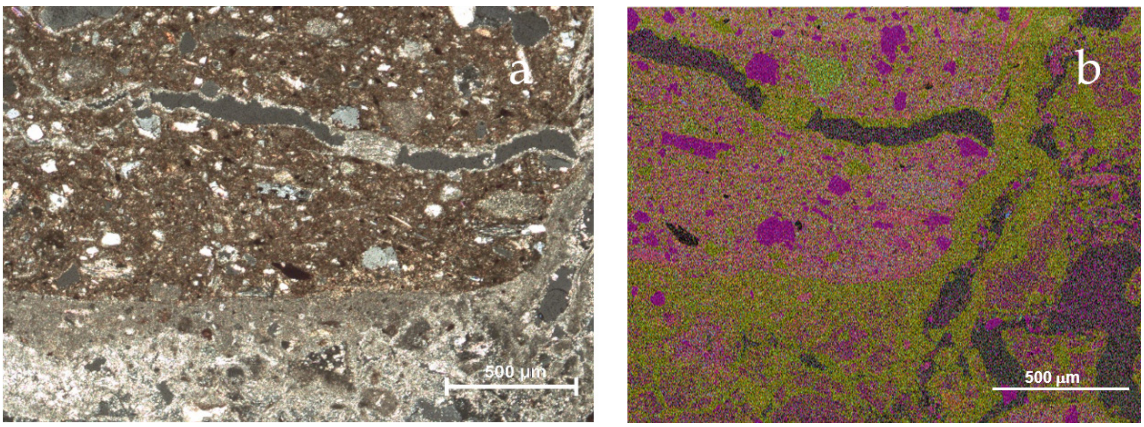

Figure 6. Microphotographs of crushed brick in a bedding mortar of the wall set against the *cella* in Building A of Sanctuary of Apollo, in Hierapolis archaeological site, Denizli (Turkey), Proto-Byzantine age under (**a**) PLM; xpl; and (**b**) EDS layered map of Ca, Si, Al, and Mg (Ca: yellow; Si: purple; Al: orange; Mg: light blue).

Another case study concerns the bedding mortars of Camponeschi Palace (18th century) in L'Aquila [53], showing sub-rounded "clusters of red clay" of millimetric grain size, dispersed in a calcitic-magnesian lime (Figure 7a); a rim seems to be present around the cluster of clay, not confirmed by the microchemical analysis (SEM EDS), which shows a too variable amount of Ca, Al, and Si around the hypothetical "rim" (Figure 7b–d). This evidence suggests that a reaction did not occur, but the cluster of clay is simply disaggregated within the binder (Table 5), confirming the bad manufacturing technique and poor state of conservation of the mortar [53] (Figure 7a).

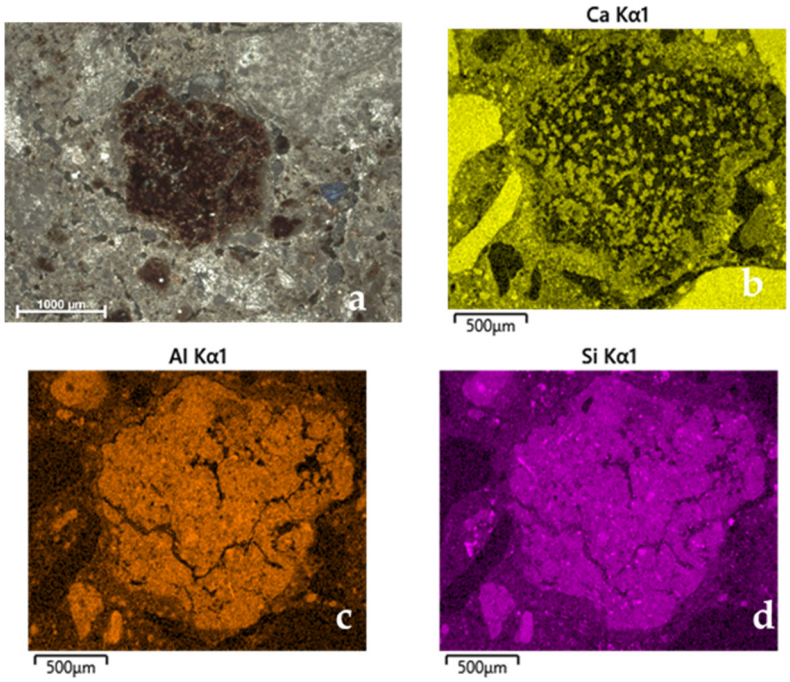

Figure 7. Microphotographs of a sub-rounded cluster of red clay in a bedding mortar of Camponeschi Palace (18th century) in L'Aquila under (**a**) PLM, xpl, and (**b**) EDS SEM map of Ca; (**c**) EDS SEM map of Al; and (**d**) EDS SEM map of Si.

Table 5. Microchemical spot analyses of rim portions of binder of Hierapolis and L'Aquila samples.

Oxides %	Hierapolis Rim 1	Hierapolis Rim 2	L'Aquila Rim 1	L'Aquila Rim 2	L'Aquila Rim 3
Na_2O	0.54	bdl	bdl	bdl	bdl
MgO	2.07	3.79	12.41	1.06	22.10
Al_2O_3	4.70	5.35	11.32	0.47	10.46
SiO_2	13.20	13.94	18.39	bdl	34.88
SO_3	1.49	1.16	bdl	0.47	bdl
K_2O	1.10	bdl	0.55	bdl	0.66
CaO	74.94	72.17	55.60	98.47	26.76
Fe_2O_3	1.73	3.58	1.33	bdl	4.55

bdl: below detection limit.

According to the literature data [7,48], if reaction rims did not develop, hydraulic phases dispersed in the binder can nevertheless still be observed both as veins and as pore filling. This can be explained by a dissolution of silica and alumina dispersed in the binder and subsequent reaction with Ca hydroxide.

Normally, the materials providing hydraulic characteristics are easily recognizable under the optical microscope and, if added finely ground, they can give rise to particular structures of the binder, as in the case of diatomaceous earth, which develops optical characteristics similar to those of microcrystalline silica, namely a micritic texture with grey of the first order interference colors. This optical feature can be observed in the PLM image of an area of unmixed binder of a waterproofing mortar of a Roman tank in Carsulæ (Terni, Italy, 1st century AD) (Figure 8a). In this case, the microchemical analysis (Figure 8b) shows high values of Si (an average around the 50%) widely spread in this portion of binder (Table 6), confirming the addition of microcrystalline silica of diatomaceous earth able to provide hydraulicity (HI range from 2.04 to 0.58).

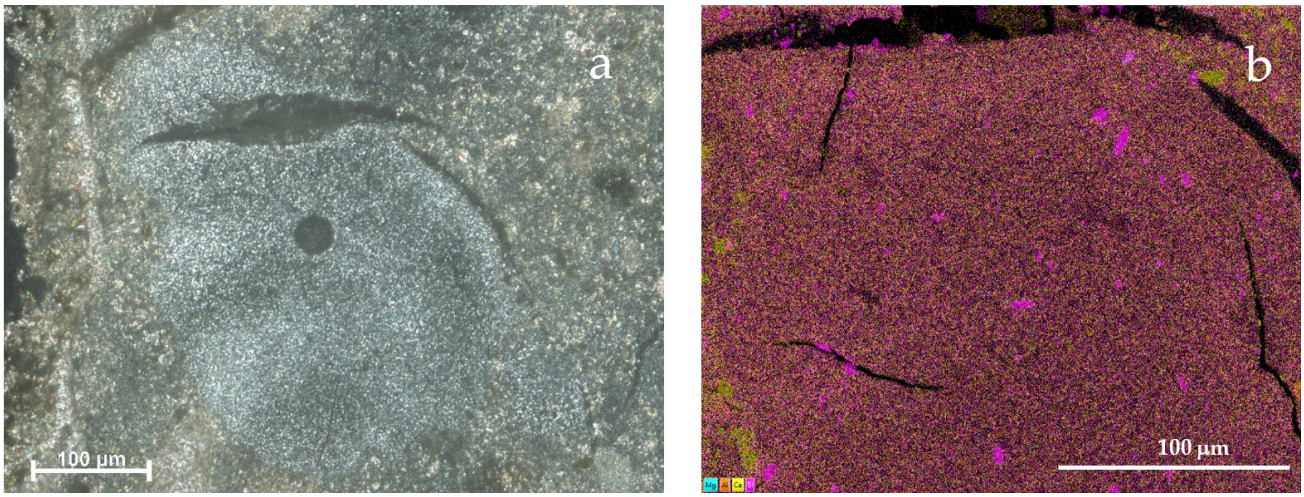

Figure 8. Microphotographs of binder of a waterproofing mortar of a Roman tank in Carsulæ (Terni, Italy, 1st century AD); (**a**) under PLM, xpl, and (**b**) SEM EDS layered map of Mg, Al, Ca, and Si (Mg: light blue; Al: orange; Ca: yellow; Si: pink).

Table 6. Microchemical spot analyses of unmixed binder of a mortar coming a waterproofing mortar of a Roman tank in Carsulæ (Terni, Italy, 1st century AD).

Oxides %	Carsulae 1	Carsulae 2	Carsulae 3	Carsulae 4	Carsulae 5
Na_2O	bdl	0.46	bdl	bdl	bdl
MgO	bdl	0.44	bdl	bdl	bdl
Al_2O_3	7.11	4.77	3.57	5.55	4.85
SiO_2	59.06	40.13	33.10	44.44	36.95
CaO	32.57	53.79	62.93	49.14	57.68

bdl: below detection limit.

3.4. Historical Natural Hydraulic Lime

As mentioned above, natural hydraulic binders are obtained by burning at temperatures of about 800−950 °C marly limestones, or siliceous limestones, setting and hardening both through carbonation of calcium hydroxide and through hydration of calcium silicates and calcium aluminates (CA, CS, C2S, and C3A) [7,8,54]. The evidence of the hydraulicity of a natural hydraulic binder is given by the presence of small dark inclusions that can be easily recognized. These inclusions could be referred to as non-hydrated relicts of belite (C2S). Belite is represented by dark brown crystals, medium-high relief, shaded contours, and subidiomorphic habitus. Such inclusions are visible in Figure 9a,b, which refer to bedding mortars of the Trebbio castle tower, located in Mugello, near Florence (15th century) and of Palazzo Davanzati (14th century, Florence) (Figure 10a,b). Previous studies [7,43] revealed that the binder of these mortars was obtained by burning a marly variety of Pietra Alberese, which contains an amount of clay minerals between 6.5 and 20%, which allowed to obtain a hydraulic lime traditionally called "strong lime". A great variability in the amount of SiO_2 and CaO was identified when analysing these areas, after identification in SEM EDS maps. Figure 9c–e refer to the SEM EDS map of Ca, Si, and Al for the binder of mortar of the Trebbio castle tower, and Figure 10c–e to Palazzo Davanzati.

For the mortar coming from Trebbio castle tower, three different binder compositional ranges were identified in the SEM EDS maps, corresponding to areas with different grey tones in BS observation:

1. The first one (spots analyses 1–5, light grey) with a composition 70.04% < CaO < 78.55%; 16.15% < SiO_2 < 24.38%; 0.72% < Al_2O_3 < 1.32% (Table 7);
2. The second one (spot analyses 6–8, dark grey) with 10.86% < CaO < 25.91%; 50.18% < SiO_2 < 54.81%; 6.01% < Al_2O_3 < 11.02% (Table 7);

3. The third one (spot analyses 9–13, grey) with 44.69% < CaO < 64.5%; 19.88% < SiO_2 < 36.35%; 2.3%; 2.3% < Al_2O_3 < 10.52% (Table 8).

Similar results were obtained for the mortar of Palazzo Davanzati where the dark grey areas (spot analyses 1–3) showed a high amount of SiO_2 and Al_2O_3 with respect to the light grey areas (spot 4–7) (see Table 9).

This microchemical variability can be produced by segregation phenomena between the clayey and calcitic portion of the marly limestone during the slaking of the quick lime, aging, and subsequent realization of the mortar mix.

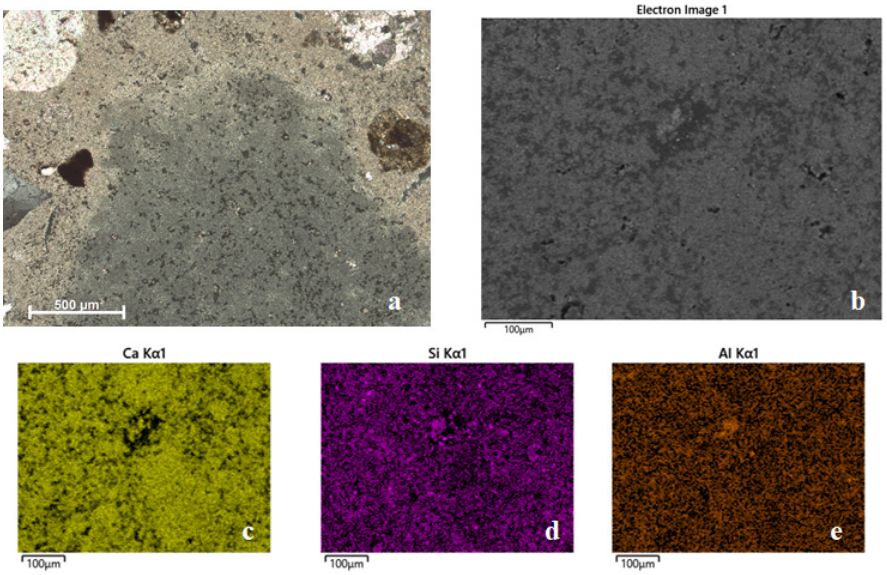

Figure 9. Microphotographs of small dark inclusions in the binder of a bedding mortar of the Trebbio castle tower, located in Mugello, near Florence (15th century); (**a**) under PLM, xpl; (**b**) BS image of a particular of this binder portion in which areas with different grey tones can be observed; (**c**) SEM EDS map of Ca; (**d**) SEM EDS map of Si; and (**e**) SEM EDS map of Al.

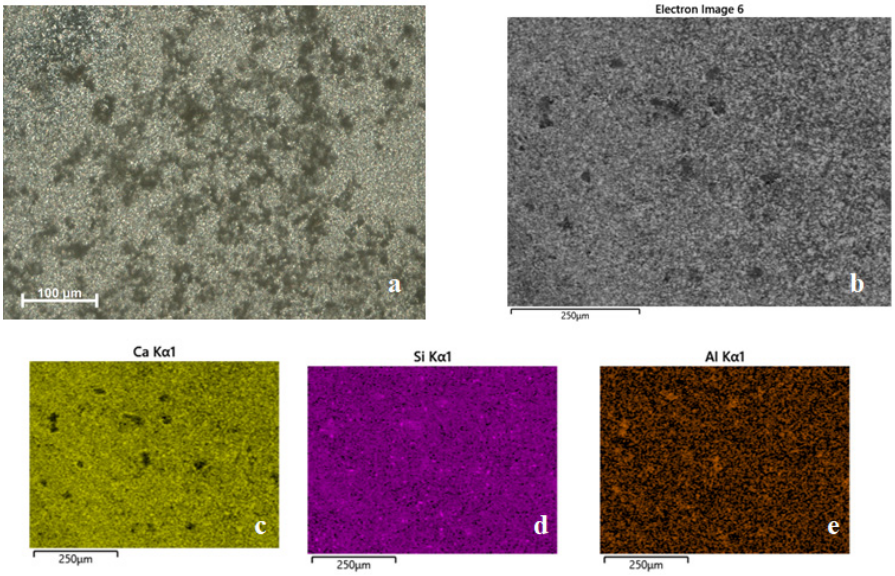

Figure 10. Microphotographs of small dark inclusions in the binder of a bedding mortar of the Palazzo Davanzati (Florence, 14th century); (**a**) under PLM, xpl; (**b**) BS image of a particular of this binder portion in which areas with different grey tones can be observed; (**c**) SEM EDS map of Ca; (**d**) SEM EDS map of Si; and (**e**) SEM EDS map of Al.

Table 7. Microchemical spot analyses (spot 1–8) of binder areas of bedding mortars from the Trebbio castle tower (Mugello, Florence).

Oxides %	Spot 1	Spot 2	Spot 3	Spot 4	Spot 5	Spot 6	Spot 7	Spot 8
Na_2O	0.57	0.47	0.88	0.62	0.28	1.08	1.17	0.71
MgO	0.49	0.72	0.75	0.67	0.41	10.9	3.28	0.8
Al_2O_3	0.72	1.04	1.1	1.32	0.98	11.02	6.01	7.28
SiO_2	16.15	18.06	21.47	20.73	24.38	53.01	54.81	50.18
P_2O_5	bdl	bdl	bdl	bdl	bdl	bdl	bdl	9.41
SO_3	0.68	0.25	0.68	0.52	0.42	1.2	0.38	1.55
K_2O	bdl	bdl	bdl	bdl	bdl	bdl	0.69	0.72
CaO	78.55	76.42	72.17	72.29	70.04	10.86	25.91	24.03
Fe_2O_3	0.48	0.35	0.27	0.72	0.46	2.97	1.16	0.67
NiO	bdl	bdl	0.24	bdl	0.07	bdl	0.32	2.64

bdl: below detection limit.

Table 8. Microchemical spot analyses (spot 9–13) of binder areas of bedding mortars from the Trebbio castle tower (Mugello, Florence).

Oxides %	Spot 9	Spot 10	Spot 11	Spot 12	Spot 13
Na_2O	0.39	1.09	0.62	0.49	0.69
MgO	1.89	1.81	0.56	0.94	1.75
Al_2O_3	5.1	3.83	6.8	10.52	2.3
SiO_2	21.91	28.99	19.88	36.35	31.9
P_2O_5	bdl	bdl	bdl	2.38	bdl
SO_3	0.4	0.45	8.02	0.68	0.25
K_2O	bdl	bdl	bdl	0.61	bdl
CaO	64.5	53.48	46.55	44.69	59.2
Fe_2O_3	4.67	6.22	0.71	2.19	0.63
NiO	bdl	1.47	0.24	bdl	bdl

bdl: below detection limit.

Table 9. Microchemical spot analyses of binder areas of from bedding mortar of Palazzo Davanzati (Florence).

Oxides %	Spot 1	Spot 2	Spot 3	Spot 4	Spot 5	Spot 6	Spot 7
Na_2O	1.52	0.56	0.97	0.45	0.69	0.8	0.27
MgO	1.60	0.43	1.02	0.82	0.81	0.94	0.43
Al_2O_3	23.31	3.98	18.82	0.95	0.64	0.74	0.34
SiO_2	42.8	38.89	41.53	8.43	7.69	9.63	5.40
P_2O_5	1.01	1.06	0.39	0.75	0.58	0.52	bdl
SO_3	bdl	bdl	bdl	bdl	bdl	bdl	0.51
K_2O	1.42	0.51	1.14	0.31	bdl	bdl	bdl
CaO	23.9	51.2	30.8	87.16	88.63	86.17	92.97
Fe_2O_3	2.58	2.41	3.17	0.77	0.05	0.49	0.08
NiO	0.23	bdl	0.77	0.09	bdl	0.26	bdl

bdl: below detection limit.

3.5. Lumps

In the study of historical mortars, it is important to assess the presence of fragments that macroscopically show a whitish color and sometimes an inconsistent appearance, generically defined as lumps [37,55]. These fragments suggest that the lime was produced according to the traditional technology of the "fusion" method: the quick lime clods are slaked in a tank with abundant water and the white paste obtained (lime putty) is drained

through a grating (that holds the biggest under-burnt fragments) in a pit/container where it is subjected to aging.

The observation in the thin section of lumps under PLM is fundamental in order to recognize their nature, according to the following types, and furthermore allows to obtain information about the stone used for the production of lime and suggestions regarding which phase of the manufacturing technologies was made with scarce care:

1. remnant of under-burnt fragments of the stone used for the production of lime;
2. remnant of over-burnt fragments of the stone used for the production of lime;
3. unmixed binder carbonated before mixing;
4. unmixed binder in the mixture;
5. "ghosts" of stone used for the production of lime, portions of carbonated binder with the structure of the original lime stone;
6. over-burnt lime stone fragments hydrated and carbonated after setting.

Type 1 can be referred to as a low burning temperature or non-uniform heat in the kiln or too big limestone fragments; type 2 may be owing to a high burning temperature or non-uniform heat in the kiln or inadequate grain size; and type 3 may be owing to the presence of carbonated crust over the lime putty tank. The presence of unmixed binder in the mixture (type 4) may be due to little care in the mixing process, while type 5 may be owing to inadequate burning with subsequent carbonation, and type 6 may be owing to overburnt lime stone fragments hydrated and carbonated after setting. The study of remnant of under-burnt fragments, as reported by numerous authors [47,56–59], allows to recognize the type of carbonate rock burnt in the kiln; an example is the under-burnt fragments of marly limestone (Pietra Alberese) present in a mortar of a Florentine county house of the 19th century (Figure 11a), the under-burnt marble fragments such as in the bedding mortars of the Roman theatre of Luni (1st century AD) (Figure 11c), and travertine of bedding mortar of Ambulatio of Torraccia di Chiusi archaeological site (second half of 4th century AD) (Figure 11d). The identification of unmixed binder in the mixture (Figure 11e) can also be very useful for dating mortars with the radiocarbon method, as it allows to avoid the procedure of separation of binder from aggregate [29,60–63]. The presence of burnt limestone fragments hydrated and carbonated after setting (Figure 11f) (in Italy, named *bottaccioli* and *calcinaroli*) can give information about the risk of decay of mortars and plasters that contains them, because they can cause physico-mechanical stress in the masonry.

The SEM observation and analyses on the lumps can be a further confirmation of the binder composition (in Figure 11b, the SEM EDS map of Ca and Si of a lump belonging to an under-burnt marly limestone of Pietra Alberese fragment shows the presence of well-preserved structures such as pure calcite veins).

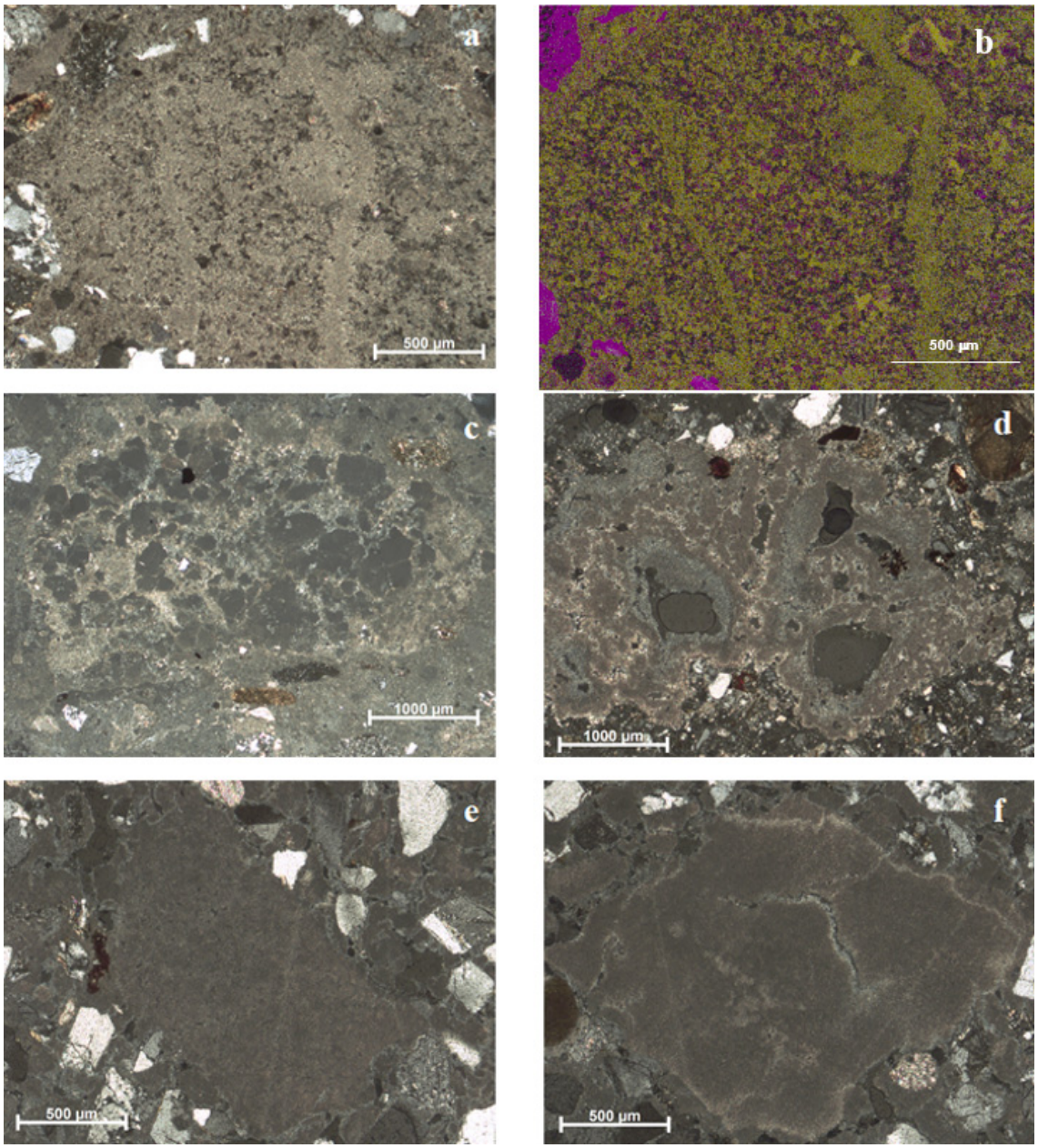

Figure 11. Microphotographs of different type of lumps: (Figure 11a,c–f, are under PLM, xpl) (**a**) under-burnt fragment of marly limestone (Pietra Alberese) from a mortar of a Florentine county house of (19th century); (**b**) SEM EDS layered map (Ca: yellow, Si: pink) of the same under-burnt fragment of Pietra Alberese; (**c**) under-burnt marble fragment in the bedding mortar of the Roman theatre of Luni (1st century AD); (**d**) under-burnt fragment of travertine from a bedding mortar of Ambulatio of Torraccia di Chiusi archaeological site (second half of 4th century AD); (**e**) unmixed binder in a mortar from San Francesco Church (Pisa) 13th–17th century; and (**f**) burnt limestone fragment hydrated and carbonated after setting from San Francesco Church (Pisa) 13th–17th century.

3.6. PLM versus SEM Observations

In the observations of the thin sections under the microscope in polarized transmitted light, the micritic/microsparitic binder may show different characteristics:

- second-order birefringence colors;
- opacity;
- of the first-order birefringence colors.

To understand this evidence, the coupling of PLM with SEM EDS seems to be the better solution. Indeed, sometimes, the problems can be due to the realization of the thin sections for the PLM observations or to the presence of different constituents inside the binders, and only the complementarity of these two analytical methodologies can be decisive. The second-order birefringence color can be due to a greater section thickness, while the opacity can be attributed to too thin thickness of section. The grey color of a lime binder may depend on a too thin section, by the presence of micro-crystalline silica (see Figure 8a,b) or by different porosity in the binder. The latter seems be the case of mortars coming from a Roman aqueduct, in Quarto (Florence), and of a bedding mortar from Spello (Figure 12a,b), in which the areas of binder with different birefringence colors (grey) were not characterized by differences in microchemical composition, as evidenced with SEM EDS analyses (Figure 12c), confirming the hypothesis that the grey color is due to a different porosity.

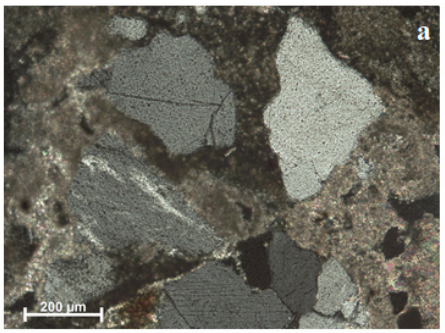

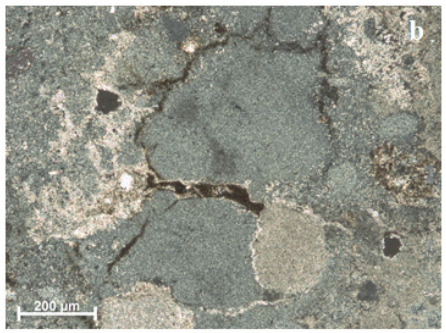

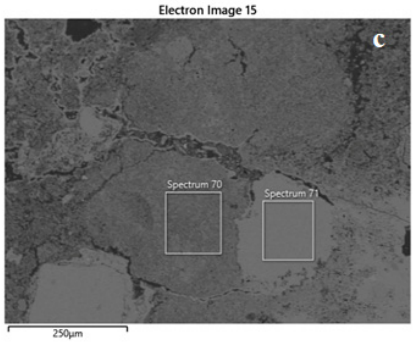

Oxide %	Spectrum 70	Spectrum 71
Na_2O	0.71	0.63
MgO	0.36	0.27
Al_2O_3	0.13	bdl
SiO_2	2.31	0.47
SO_3	0.56	0.24
CaO	95.55	98.32
FeO	0.39	0.07
NiO	bdl	bdl

Figure 12. Microphotographs of the binder of a bedding mortar of a Roman aqueduct (Quarto-Florence) with grey areas; (**a**) under PLM, xpl; (**b**) particular of an area of binder of a bedding mortar of Roman findings (Spello, Perugia, Italy) with different birefringence color under PLM, xpl; and (**c**) BS SEM image of same area of (**b**) and micro chemical analyses of selected areas in the previous image.

4. Conclusions

In this paper, the advances in the use of minero-petrographic observations combined with SEM EDS analyses in the study of historical mortars and their binder are described.

As known PLM is a methodology able to furnish a large amount of information about the different types of mortars through the characterization of binder, aggregate, porosity, decay phenomena, and so on, together with a considerable cost-effectiveness of investigation. The coupling of PLM analyses with SEM EDS technique, in the case of analyses of binder, can provide further fundamental information on the texture, microstructure, and composition.

In the case of air hardening lime mortars, PLM and SEM EDS analyses allow to recognize the type of burned limestone (calcitic or dolomitic), the manufacturing technologies, and the possible dissolution/recrystallization phenomena. For ancient mortars made of air hardening calcitic lime with materials providing hydraulic characteristics, PLM observation provide information about the materials (tuff, pumice, volcanic ash, crushed bricks, and

so on) deliberately added to obtain hydraulicity, their distribution, the grain size, and the shape of grains. The coupling with SEM EDS analyses allows to confirm the presence of effective reaction between binder and the hydraulic materials, besides determining the presence of finely ground material (i.e., microcrystalline silica) able to confer higher hydraulicity to mortar. The microchemical analyses make possible to calculate the HI of binders.

For historical natural hydraulic lime, obtained by burning at temperatures of about 800–950 °C marly limestones, or siliceous limestones, the PLM observation combined with SEM EDS analyses provides information about the presence of small dark inclusions and their composition, highlighting the great variability of the composition of these binders.

In the case of the presence of lumps, the PLM observation allows their classification, in order to obtain suggestions about the stone used for the production of lime and regarding which phase of the manufacturing technologies was made with scarce care. The coupling with SEM EDS morphological and microchemical analyses gives further data on type of lumps, on their origin, and on the composition of stone burnt for the production of lime.

In addition, the chemical data can help in understanding the reason for some birefringence color variations in the binders.

In conclusion, the different characteristics of mortars, in terms of raw materials and technologies used for the preparation of mixture and application in the masonries, studied through two classic, but equally fundamental methods of investigation (PLM and SEM EDS), are able to provide precious knowledge on the history of material culture.

In addition to their cultural significance, the ancient mortars, obtained with local raw materials and traditional technologies, could provide inspiration to design compatible and durable restoration mortars.

Author Contributions: Conceptualization, E.C., F.F., and E.P.; methodology, E.C., F.F., and E.P.; validation, E.C., F.F., and E.P.; formal analysis, E.C., F.F., and E.P.; investigation, E.C., F.F., and E.P.; data curation, E.C., F.F., and E.P.; writing—original draft preparation, E.C., F.F., and E.P.; writing—review and editing, E.C., F.F., and E.P.; visualization, E.C., F.F., and E.P.; supervision, E.C., F.F., and E.P. All authors have read and agreed to the published version of the manuscript.

Funding: This research received no external funding.

Conflicts of Interest: The authors declare no conflict of interest.

References

1. Cagnana, A. I Leganti, gli Intonaci, gli Stucchi. In *Archeologia dei Materiali da Costruzione*; SAP Società Archeologica S.r.l.: Mantova, Italy, 2000; p. 248.
2. Henry, A.; Stuart, J.D. *Practical Building Conservation: Mortars, Renders & Plasters*; Ashgate: Farnham, UK, 2012; p. 654.
3. Bonazzi, A.; Fieni, L. *Uso e Fortuna delle Malte D'Argilla Nell'Italia Settentrionale: Prime Ricerche su Cremona*; TeMa: Cagliari, Italy, 1995; p. 52.
4. Crisci, G.M.; Franzini, M.; Lezzerini, M.; Mannoni, T.; Riccardi, M.P. Ancient mortars and their binder. *Period. Di Miner.* **2004**, *73*, 259–268.
5. Artioli, G. Let the walls speak. A brief history of binders in architecture. In *Rendiconti Accademia Nazionale delle Scienze detta dei XL Memorie di Scienze Fisiche e Naturali*; Libreria Universitaria: Roma, Italy, 2017; Volume XLI, Parte II, Tomo I; pp. 7–18.
6. Costa, C. Hydraulic Binder. In *Materials for Construction and Civil Engineering*; Gonaçalves, M.C., Margarido, F., Eds.; Springer: Cham, Switzerland, 2015; pp. 1–52.
7. Pecchioni, E.; Fratini, F.; Cantisani, C. *Le Malte Antiche e Moderne tra Tradizione e Innovazione*, 2nd ed.; Pàtron: Bologna, Italy, 2018; p. 231.
8. Pecchioni, E.; Fratini, F.; Cantisani, E. *Atlas of the Ancient Mortars in Thin Section under Optical Microscope*, 2nd ed.; Nardini: Florence, Italy, 2020; p. 78.
9. Jedrzejewska, H. Old mortars in Poland: A new method of investigation. *Stud. Conserv.* **1960**, *5*, 132–138.
10. Cliver, E.B. Tests for analysis of mortar samples. *Bull. Assoc. Preserv. Technol.* **1974**, *6*, 68–73. [CrossRef]
11. Frizot, M. L'analyse des mortiers antiques; problèmes et résultat. In *Mortars, Cements and Grouts used in the Conservation of Historic Building, Proceedings of the ICCROM Symposium, Rome, Italy, 3–6 November 1981*; Iccrom: Rome, Italy, 1981; pp. 331–341.
12. Dupas, M. L'analyse des mortiers et enduits des peintures murales et des bâtiments anciens. In *Mortars, Cements and Grouts Used in the Conservation of Historic Building, Proceedings of the ICCROM Symposium, Roma, Italy, 3–6 November 1981*; Iccrom: Rome, Italy, 1981; pp. 281–295.

13. Franchi, R.; Fratini, F.; Manganelli Del Fà, C. Caratterizzazione degli Intonaci mediante l'impiego di tecniche Mineralogico-Petrografiche. In *L' Intonaco: Storia, Cultura e Tecnologia, Proceedings of the Conference Scienza e Beni Culturali, Bressanone, Italy, 24–27 June 1985*; Libreria Progetto: Padova, Italy, 1985; pp. 167–183.
14. Middendorf, B.; Baronio, G.; Callebaut, K.; Huges, J.J. Chemical mineralogical and physical-mechanical investigations of old mortars. In *Historic Mortars: Characteristics and Tests, Proceedings of the RILEM TC-167COM International Workshop, Paisley, Scotland, 12–14 May 1999*; Bartos, P., Groot, C., Hughes, J.J., Eds.; Chapman & Hall: London, UK, 2000; pp. 53–61.
15. Van Balen, K.; Toumbakari, E.E.; Blanco Varela, M.T.; Aguilera, J.; Puertas, F.; Sabbioni, C.; Zappia, G.; Riontino, C.; Gobbi, G. Procedure for a mortar type identification: A proposal. In *Historic Mortars: Characteristics and Tests, Proceedings of the RILEM TC-167COM International Workshop, Paisley, Scotland, 12–14 May 1999*; Bartos, P., Groot, C., Hughes, J.J., Eds.; Chapman & Hall: London, UK, 2000; pp. 61–79.
16. Martinet, G.; Quenée, B. Proposal for a useful methodology for the study of ancient mortars. In *Historic Mortars: Characteristics and Tests, Proceedings of the RILEM TC-167COM International Workshop, Paisley, Scotland, 12–14 May 1999*; Bartos, P., Groot, C., Hughes, J.J., Eds.; Chapman & Hall: London, UK, 2000; pp. 81–91.
17. Matteini, M.; Moles, A. *Scienza e Restauro: Metodi di Indagine*; Nardini: Firenze, Italy, 1984; p. 316.
18. Amoroso, G.; Camaiti, M. Scienza dei materiali e restauro. In *La Pietra: Dalle mani Degli Artisti e Degli Scalpellini a quelle dei Chimici Macromolecolari*; Alinea: Firenze, Italy, 1997; p. 328.
19. Pecchioni, E. Le malte impiegate nel patrimonio culturale: Caratterizzazione e conservazione. *Plinius Suppl. Eur. J. Miner.* **2000**, *23*, 214–221.
20. Weber, J.; Köberle, T.; Pintér, F. Methods of microscopy to identify and characterise hydraulic binders in historic mortars—A methodological approach. In Proceedings of the 3rd Historical Mortar Conference, Glasgow, UK, 11–14 September 2013; pp. 1–8.
21. Arizzi, A.; Cultrone, G. Mortars and plasters-how to characterize hydraulic mortars. *Archaeol. Anthr. Sci.* **2021**, *13*, 2–22.
22. Elert, K.; Rodriguez-Navarro, C.; Sebastian Pardo, E.; Hansen, E.; Cazallo, O. Lime mortars for the conservation of historic buildings. *Stud. Conserv.* **2002**, *47*, 62–75.
23. Lugli, S.; Caroselli, M.; Marchetti Dori, S.; Vandelli, V.; Marzani, G.; Segattini, R.; Bianchi, C.; Weber, J. Building materials and degradation phenomena of the Finale Emilia Town Hall (Modena): An archaeometric study for the restoration project after the 2012 earthquake. 2016 Period. *Di Miner.* **2016**, *85*, 59–67.
24. Ponce-Anton, G.; Arizzi, A.; Zuluaga, M.C.; Cultrone, G.; Ortega, L.A.; Mauleon, J.A. Mineralogical, textural and physical characterisation to determine deterioration susceptibility of Irulegi Castle lime mortars (Navarre, Spain). *Materials* **2019**, *12*, 584. [CrossRef] [PubMed]
25. Coutelas, A.; Guyard, L.; David, C.H. Pétroarchéologie de mortiers gallo-romains: Application de méthodes analytiques à l'étude des thermes du Vieil-Evreux (Eure). In *Les Nouvelles de l'Archéologie*; Giligny, F., Ed.; Éditions de la Maison des Sciences de L'homme: Paris, France, 2000; Volume 81, pp. 31–36.
26. Quaresima, R. Lo studio e la caratterizzazione delle malte: Contributo imprescindibile all'archeologia? Stratigrafia degli elevati e nuove tecniche diagnostiche. In *Archeologia dell'Edilizia Storica in Situazioni di Emergenza*; Redi, F., Forgione, A., Armillotta, F., Eds.; One Group: L'Aquila, Italy, 2017; pp. 105–127.
27. Miriello, D.; Bloise, A.; Crisci, G.M.; De Luca, R.; De Nigris, B.; Martellone, A.; Osanna, M.; Pace, R.; Pecci, A.; Ruggieri, N. New compositional data on ancient mortars and plasters from Pompeii (Campania—Southern Italy): Archaeometric results and considerations about their time evolution. *Mater. Charact.* **2018**, *146*, 189–203. [CrossRef]
28. Secco, M.; Previato, C.; Addis, A.; Zago, G.; Kamsteeg, A.; Dilaria, S.; Canovaro, C.; Artioli, G.; Bonetto, J. Mineralogical clustering of the structural mortars from the Sarno Baths, Pompeii: A tool to interpret construction techniques and relative chronologies. *J. Cult. Herit.* **2019**, *40*, 265–273. [CrossRef]
29. Cantisani, E.; Calandra, S.; Barone, S.; Caciagli, S.; Fedi, M.; Garzonio, C.A.; Liccioli, L.; Salvadori, B.; Salvatici, T.; Vettori, S. The mortars of Giotto's Bell Tower (Florence, Italy): Raw materials and technologies. *Constr. Build Mater.* **2021**, *267*, 120801. [CrossRef]
30. Rodriguez-Navarro, C.; Ruiz-Agudo, E.; Ortega-Huertas, M.; Hansen, E. Nanostructure and Colloidal Behavior of Ca(OH)2: Implications for the Conservation of Cultural Heritage. *Langmuir* **2005**, *21*, 10948–10957. [CrossRef] [PubMed]
31. Jackson, M.D.; Chae, S.R.; Mulcahy, S.R.; Meral, C.; Taylor, R.; Penghui, L.; Emwas, A.H.; Moon, J.; Seyoon, Y.; Vola, G.; et al. Unlocking the Secrets of Al-tobermorite in Roman Seawater Concrete. *Am. Mineral.* **2013**, *98*, 1669–1687. [CrossRef]
32. Bertrand, L.; Gervais, C.; Masic, A.; Robbiola, L. Paleo-inspired systems: Durability, sustainability, and remarkable properties. Angew. *Chem. Int.* **2018**, *25*, 7288–7295. [CrossRef] [PubMed]
33. Maragh, J.M.; Weaver, J.C.; Masic, A. Large-scale micron-order 3D surface correlative chemical imaging of ancient Roman concrete. *PLoS ONE* **2019**, *14*, e0210710. [CrossRef] [PubMed]
34. Fratini, F.; Rescic, S.; Cantisani, E.; Pecchioni, E.; Pasolini, S.; Cagnini, A. A new mortar from a strange ancient mortar. In Proceedings of the IMEKO TC-4 International Conference on Metrology for Archaeology and Cultural Heritage, Florence, Italy, 4–6 December 2019; pp. 454–458.
35. Zhang, K.; Sui, Y.; Wang, L.; Tie, F.; Yang, F.; Liu, Y.; Zhang, Y. Effects of sticky rice addition on the properties of lime tile dust mortars. *Herit. Sci.* **2021**, *9*, 4. [CrossRef]
36. Oliveira, A.; Pereira, A.; Lemos, P.C.; Guerra, J.P.; Silva, V.; Faria, P. Effect of innovative bio products on a lime mortars. *J. Build. Eng.* **2021**, *35*, 101985. [CrossRef]
37. Bugini, R.; Toniolo, L. La presenza di grumi bianchi nelle malte antiche: Ipotesi sull'origine. *Arkos* **1990**, *12*, 4–8.

38. Bruni, S.; Cariati, F.; Fermo, P.; Cairati, P.; Alessandrini, G.; Toniolo, L. White lumps in fifth- to seventeenth-century A.D. mortars from Northern Italy. *Archaeometry* **1997**, *39*, 1–7. [CrossRef]
39. Elsen, J.; Brutsaert, A.; Deckers, M.; Brulet, R. Microscopical study of ancient mortars from Tournai (Belgium). *Mater. Charact.* **2004**, *53*, 289–294. [CrossRef]
40. Pouchou, J.L.; Pichoir, F. Quantitative Analysis of Homogeneous or Stratified Microvolumes Applying the Model "PAP". In *Electron Probe Quantitation*; Springer: Boston, MA, USA, 1991; pp. 31–75.
41. Cantisani, E.; Cecchi, A.; Chiaverini, J.; Fratini, F.; Manganelli Del Fa, C.; Pecchioni, E.; Rescic, S. The binder of the "Roman Concrete" of the Ponte di Augusto in Narni (Italy). Period. *Di Miner.* **2002**, *71*, 113–123.
42. Fratini, F.; Arrighetti, A.; Cantisani, E.; Pecchioni, E. I materiali da costruzione della Fortezza di San Martino a San Piero a Sieve (Toscana, Italia). In *Defensive Architecture of the Mediterranean*; Marotta, A., Spallone, R., Eds.; Politecnico di Torino: Turin, Italy, 2018; Volume VII, pp. 381–388.
43. Fratini, F.; Cantisani, E.; Pecchioni, E.; Pandeli, E.; Vettori, S. Pietra Alberese: Building Material and Stone for Lime in the Florentine Territory (Tuscany, Italy). *Heritage* **2020**, *3*, 1520–1538. [CrossRef]
44. Sánchez-Moral, S.; Luque, L.; Cañaveras, J.C.; Soler, V.; Garcia-Guinea, J.; Aparicio, A. Lime-pozzolana mortars in Roman catacombs: Composition, structures and restoration. *Cem. Concr. Res.* **2005**, *35*, 1555–1565. [CrossRef]
45. Velosa, A.L.; Veiga, R.; Coroado, J.; Ferreira, V.M.; Rocha, F. Characterization of Ancient Pozzolanic Mortars from Roman Times to the 19th Century: Compatibility Issues of New Mor-tars with Substrates and Ancient Mortars. In *Materials, Technologies and Practice in Historic Heritage Structures*; Dan, M.B., Pikryl, R., Török, Á., Eds.; Springer: Dordrecht, Germany, 2010; pp. 235–257.
46. Naga Sai, A.; Ramadoss, R. A review on role of additives & pozzolanic materials in ancient structures. *Mater. Today Proc.* **2021**, *43*, 1383–1388.
47. Pavia, S. A petrographic study of mortar hydraulicity. In Proceedings of the HMC 08—1st Historical Mortar Conference, Lisboa, Portugal, 24–28 September 2008.
48. Moropoulu, A.; Cakmak, A.S.; Biscontin, G.; Bakolas, A.; Zendri, E. Advanced Byzantine cement based composites resisting earthquake stress: The crushed brick/lime mortars of Justinian's Hagia Sophia. *Constr. Build. Mater.* **2002**, *16*, 543–552. [CrossRef]
49. Massazza, F. Pozzolana and pozzolanic cements. In *Lea's Chemistry of Cement and Concrete*; Hewlett, P.C., Ed.; Elsevier: London, UK, 2007; pp. 471–602.
50. St John, D.A.; Poole, A.W.; Sims, I. *Concrete Petrography*; Arnold: London, UK, 1998; p. 488.
51. Charola, E.; Henriques, F. Hydraulicity in lime mortars revisited. In *Historic Mortars: Characteristics and Tests, Proceedings of the RILEM TC-167COM International Workshop, Paisley, Scotland, 12–14 May 1999*; Bartos, P., Groot, C., Hughes, J.J., Eds.; Chapman & Hall: London, UK, 2000; pp. 97–106.
52. Cantisani, E.; Vettori, S.; Ismaelli, T.; Scardozzi, G. Imperial age mortars at Hierapolis: Raw materials and technologies. In *Ancient Quarries and Building Sites in Asia Minor. Research on Hierapolis in Phrygia and other Cities in South-Western Anatolia: Archaeology, Archaeometry, Conservation*; Ismaelli, T., Scardozzi, G., Eds.; Edipuglia: Bari, Italy, 2016; pp. 589–608.
53. Pecchioni, E.; Quaresima, R.; Fratini, F.; Cantisani, E. Importance of Mortars Characterization in the structural behaviour of Monumental and Civil Buildings: Case Histories in L'Aquila (Italy). In *Engineering Geology for Society and Territory-Preservation of Cultural Heritage*; Lollino, G., Giordan, D., Crosta, G.B., Corominas, J., Azzam, R., Wasowski, J., Sciarra, N., Eds.; Springer International: Cham, Switzerland, 2015; Volume 8, pp. 387–391.
54. Ingham, J. *Geomaterials under the Microscope: A Colour Guide*; John Wiley & Sons: Hoboken, NJ, USA, 2010; p. 192.
55. Secco, M.; Dilaria, S.; Addis, A.; Bonetto, J.; Artioli, G.; Salvadori, M. The Evolution of the Vitruvian Recipes over 500 Years of Floor-Making Techniques: The Case Studies of the Domus delle Bestie Ferite and the Domus di Tito Macro (Aquileia, Italy). *Archeometry* **2018**, *60*, 185–206. [CrossRef]
56. Fratini, F.; Pecchioni, E.; Cantisani, C. The petrographic study in the ancient mortar characterisation. In Proceedings of the HMC 08—1st Historical Mortar Conference, Lisboa, Portugal, 24–28 September 2008; pp. 1–8.
57. Hughes, J.J.; Leslie, A.B. The petrography of lime inclusions of historic lime based mortars. In Proceedings of the 8th Euroseminar on Microscopy applied to building materials, Athens, Greece, 4–7 September 2001; Georgali, B., Toumbakari, E., Eds.; pp. 359–364.
58. Leslie, A.B.; Hughes, J.J. Binder microstructure in lime mortars: Implications for the interpretation of analysis results. *Q. J. Eng. Geol. Hydrogeol.* **2002**, *53*, 257–263. [CrossRef]
59. Pavía, S.; Caro, S. Lime mortars for masonry repair: Analytical science and laboratory testing versus practical experience. In *Theory and Practice in Conservation—A tribute to Cesare Brandi, Proceedings of the International Seminary, Lisboa, Portugal, 12–14 May 2006*; Delgado Rodrigues, J., Mimoso, J.M., Eds.; Laboratorio Nacional de Engenharia Civil: Lisboa, Portugal, 2006; pp. 493–500.
60. Heinemeier, J.; Jungner, H.; Lindroos, A.; Ringbom, Å.; Von Konow, T.; Rud, N. AMS 14C dating of lime mortar. *Nucl. Instrum. Methods Phys. Res. Sect. B Beam Interact. Mater. At.* **1997**, *123*, 487–495. [CrossRef]
61. Pesce, G.; Quarta, G.; Calcagnile, L.; D'elia, M.; Cavaciocchi, P.; Lastrico, C.; Guastella, R. Radiocarbon dating of lumps from aerial lime mortars and plasters: Methodological issues and results from San Nicolò of Capodimonte Church (Camogli, Genoa, Italy). *Radiocarbon* **2009**, *51*, 867–872. [CrossRef]
62. Lindroos, A.; Ranta, H.; Heinemeier, J.; Lill, J.O. 14C chronology of the oldest Scandinavian church in use. *An AMS/PIXE study of lime lump carbonate in the mortar. Nucl. Instrum. Methods Phys. Res. B* **2014**, *331*, 220–224. [CrossRef]
63. Addis, A.; Secco, M.; Marzaioli, F.; Artioli, G.; Arnau, A.C.; Passariello, I.; Terrasi, F.; Brogiolo, G.P. Selecting the most reliable 14Cdating material inside mortars: The origin of the Padua Cathedral. *Radiocarbon* **2019**, *61–62*, 375–393. [CrossRef]